Title

U-insertion/deletion RNA editing multiprotein complexes and mitochondrial ribosomes in Leishmania tarentolae are located in antipodal nodes adjacent to the kinetoplast DNA

Authors

Wong, Richard G
Kazane, Katelynn
Maslov, Dmitri A
et al.

Publication Date

2015-11-01

DOI

10.1016/j.mito.2015.10.006

Peer reviewed

HHS Public Access

Author manuscript

Mitochondrion. Author manuscript; available in PMC 2016 November 01.

Published in final edited form as:

Mitochondrion. 2015 November ; 25: 76–86. doi:10.1016/j.mito.2015.10.006.

U-INSERTION/DELETION RNA EDITING MULTIPROTEIN COMPLEXES AND MITOCHONDRIAL RIBOSOMES IN *LEISHMANIA TARENTOLAE* ARE LOCATED IN ANTIPODAL NODES ADJACENT TO THE KINETOPLAST DNA

Richard G Wong[1,5], **Katelynn Kazane**[2,5], **Dmitri A Maslov**[3], **Kestrel Rogers**[4], **Ruslan Aphasizhev**[6], and **Larry Simpson**[5,*]

[1]Department of Gerontology, Davis School of Gerontology, University of Southern California, Los Angeles, CA 90089

[2]Multispan Inc., Hayward, CA 94544

[3]Department of Biology, University of California - Riverside, Riverside, CA 92521

[4]Department of Botany and Plant Sciences, Institute of Integrative Genome Biology, University of California, Riverside, CA, 92521[5]

[5]Department of Microbiology, Immunology and Molecular Genetics, Geffen School of Medicine at UCLA, Los Angeles, CA 90095

[6]Department of Molecular and Cell Biology, Boston University School of Dental Medicine, Boston, MA 02118

Abstract

We studied the intramitochondrial localization of several multiprotein complexes involved in U-insertion/deletion RNA editing in trypanosome mitochondria. The editing complexes are located in one or two antipodal nodes adjacent to the kinetoplast DNA (kDNA) disk, which are distinct from but associated with the minicircle catenation nodes. In some cases the proteins are in a bilateral sheet configuration. We also found that mitoribosomes have a nodal configuration. This type of organization is consistent with evidence for protein and RNA interactions of multiple editing complexes to form a ~40S editosome and also an interaction of editosomes with mitochondrial ribosomes.

Keywords

Leishmania; RNA; editing; antipodal node; trypanosome; kinetoplast

[*]Corresponding author: larrys3255@gmail.com (Larry Simpson).

1. Introduction

Leishmania represents a genus within the monophyletic kinetoplastid order, Trypanosomatida, which contains both parasitic and free-living organisms. The term, trypanosomatid, is generally used to designate a member of this order. Trypanosomatids belong to the group, Kinetoplastida, which are characterized by an unusual mitochondrial DNA known as kinetoplast DNA, which consists of *Leishmania sp*. are the causal agents of a number of important human and animal diseases. *Leishmania* of reptiles are closely related to the pathogenic trypanosomatids (Couvreur, 2013; Fraga et al., 2010; Kang et al., 2006; Simpson et al., 2006). *L. tarentolae* was isolated from the gecko, *Tarentolae mauritanica*, by Parrot in Algeria in 1939, and maintained in culture in various laboratories for many years (Simpson et al., 2015). These cells are non-pathogenic for mammals (Taylor et al., 2010) and grow readily in Brain Heart Infusion (BHI) (Difco) at 27˚C with hemin added to 10 μg/ml (Simpson et al., 1970). *L. tarentolae* has been studied extensively as a model trypanosomatid and has been recently developed and commercialized as a useful eukaryotic expression vector (Basile and Peticca, 2009; Breitling et al., 2002; Dortay and Mueller-Roeber, 2010; Fritsche et al., 2007; Klatt and Konthur, 2012; Kovtun et al., 2010; Kushnir et al., 2011; Kushnir et al., 2005).

The kinetoplast of the trypanosomatid protists was first identified as a Giemsa-stained structure located at the base of the flagellum and the actual term was proposed in 1917 by Alexeieff to substitute for the previous term “kinetonucleus” (Alexeieff, 1917). The first evidence that the kinetoplast represents a highly concentrated mass of DNA was obtained in 1927, when M. Robertson applied the then novel DNA-specific Feulgen stain to the kinetoplast of *Bodo caudatus* and *Trypanosoma rajae* (Miles, 1976). The isolated kinetoplast-mitochondrial DNA (kDNA) was shown to be a giant network of 54–20,000 catenated minicircle molecules which vary in size between species: *L. tarentolae* minicircles are ~850 bp, *Trypanosoma brucei* minicircles are ~1200 bp, *Trypanosoma cruzi* minicircles are ~1000 bp, and *Crithidia fasciculata* minicircles are ~2300 bp (Simpson and da Silva, 1971). The kDNA is condensed into a disk approximately 1 μm in diameter and 0.4 μm thick *in situ* and this disk is located within a region of the single mitochondrion adjacent to the basal body of the flagellum. The term, “kinetoplast”, is now used for the region of the mitochondrion that contains the kDNA but the word is also used for the kDNA disk itself. See Supplemental Fig. S1A for diagram of the kDNA disk and associated structures.

Each minicircle is catenated to approximately three other minicircles. The catenated minicircles are oriented perpendicular to the length of the cell. There is also a minor catenated DNA component in the network known as maxicircle DNA, which consists of around 20–30 circular molecules 20–40 kb in size, depending on the species. The maxicircle DNA encodes two small rRNAs and 18 proteins which are homologous to mitochondrial proteins in other organisms, and the genetic role of the minicircles is to encode guide RNAs (gRNAs) involved in mediating insertion/deletion of U residues, as discussed below.

Replication of the kinetoplast DNA is fairly synchronous with replication of nuclear DNA. The first indication of a mechanism for the replication of network minicircles was obtained by pulse labeling *L. tarentolae* cells with ^{3}H thymidine which showed that newly replicated

minicircles are located in two antipodal nodes adjacent to the kDNA disk. This stage is followed in a pulse-chase by the appearance of a ring of replicated open minicircles which eventually migrated to the center of the network and became distributed throughout the network after one cell division. The puzzles of kDNA replication were largely resolved by the elegant studies of Englund, who developed a model in which covalently closed minicircles are randomly released from the network by a Type II Topoisomerase (Topo II), replicated on the flagellar side of the kinetoplast and then recatenated as nicked and gapped open minicircles at the two antipodal nodes (Jensen and Englund, 2012). The appearance of a ring of replicated open minicircles and the apparent migration of these molecules towards the center is explained by rotation (*Crithidia*, *Leishmania*) or oscillation (*Trypanosoma brucei*) of the network during recatenation. The recatenated open minicircles remain nicked and gapped for the entire S phase and the gaps are fairly simultaneously repaired in early G_2. The observed redistribution of the minicircles after one cell cycle (Simpson et al., 1974) results from the random decatenation, replication and recatenation of open minicircles at different sites around the circumference during S phase. See Supplemental Fig. S1A for a diagram of the replication model.

Multiple enzymes involved in DNA repair and catenation were found to co-localize to the same antipodal nodes, which we therefore term, “ repair-catenation” nodes. These include a Type II Topoisomerase (Melendy et al., 1988), DNA polymerase β (Bruhn et al., 2011; Concepcion-Acevedo et al., 2012; Klingbeil et al., 2002; Saxowsky et al., 2003; Sinha et al., 2004), DNA primases PRI1 and PRI2 (Hines a nd Ray, 2010, 2011), the TbPIF1 (Liu et al., 2010) and PIF5 helicases (Liu et al., 2009), p38 (Liu et al., 2006), p93 (Li et al., 2007) and SSE1 RNaseH (Engel and Ray, 1999). The localization of LIG kβ is nodal but not overlapping with that of Topo II, suggesting that these proteins may be contained in separate but associated complexes (Downey et al., 2004).

LIG kβ also shows localization on both sides of the kDNA disk in a minority of cells, as does the histone H1- like protein, Kap4 (Xu et al., 1996) and the helicase, TbPIF8 (Wang et al., 2012). Several DNA replication enzymes, PolIβ, PolIC and PIF2, are apparently localized in the kinetoflagellar mitochondrial matrix region opposite the distal side of the kDNA disk where replication of the decatenated closed minicircles occurs (Onn et al., 2006).

There are also two nodes on the kinetoflagellar side which contain the UMSBP protein (Abu-Elneel et al., 2001) that binds a short conserved origin of replication sequence in the minicircles. See Supplemental Figs. S1A and S1B for diagrams of the kDNA disk with the known nodal and sheet localization of enzymes involved in minicircle gap repair and catenation.

The tripartite attachment complex (TAC) consists of unilateral filaments linking the kDNA disk to a small region of the mitochondrial membrane and a set of exclusion zone filaments connecting the membrane to the basal bodies (Ogbadoyi et al., 2003). These filaments position the kDNA disk to a region of the matrix and also possibly mediate segregation of daughter kDNA networks in the cell cycle. Several TAC proteins have been so far identified

(Bonhivers et al., 2008; Lacomble et al., 2012; Schnarwiler et al., 2014; Zhao et al., 2008). See Fig. S1A for diagram of relationship of TAC complex to kDNA disk.

In addition to having an unusual mitochondrial DNA, trypanosomatids exhibit a novel post-transcriptional mRNA processing activity known as uridylate (U) insertion/deletion RNA editing in which multiple frameshifts in 12 of the 18 structural genes in the maxicircle are corrected at the RNA level. The genetic role of the kDNA minicircles is the encoding of short 3' uridylated "guide RNAs" (gRNAs) which act *in trans* by base-pairing to pre-edited mRNAs to specify the sites of U-insertion and deletion (Sturm and Simpson, 1991). The mechanism involves the formation of an RNA-RNA "anchor duplex" just downstream of the first editing site which recruits a number of multiprotein complexes. The pre-edited mRNA is cleaved at the mismatch just upstream of the anchor duplex and U residues are added to or removed from the 3' end of the 5' cleavage fragment. The edited RNA sequence base pairs with the gRNA and the two fragments are then ligated. The mature edited mRNA is adenylated and uridylated at the 3' end and this molecule interacts with the mitochondrial ribosome, thereby initiating the translation process. The number of gRNAs involved for different editing domains varies from one to more than 10. The number of different minicircle "sequence classes" as defined by encoding specific gRNAs, range in two strains of *L. tarentolae* from ~10 to almost 5,000 per network of 10,000 minicircles (Simpson et al., 2015). An overall 3' to 5' polarity of multi-gRNA-mediated editing is determined by the editing of a "block" of the transcript by the first gRNA which creates the anchor sequence for hybridization of the second gRNA, and so on (Maslov and Simpson, 1992). See Supplemental Figs. S2A and S2B for diagrams of the cleavage-ligation model of RNA editing.

The editing complexes include the RNA editing core complex or RECC, and several accessory complexes. Medium resolution structures have been obtained for the 24S RECC in *T. brucei* (Golas et al., 2009) and in *L. tarentolae* (Li et al., 2009) by cryo-electron microscopy. Blue native gel evidence for the existence of an RNase-sensitive ~40S complex that contains the RECC has been presented (Osato et al., 2009). Recently a complex protein-RNA and protein-protein interaction network of several RNA editing processing complexes to form an RNase-sensitive "40S editosome" was described (Aphasizheva et al., 2014). The RNA editing substrate binding complex (RESC) has three modules: a gRNA-binding complex (GRBC/MRB) (Hashimi et al., 2008), an RNA editing mediator complex (REMC) and a polyadenylation mediator complex (PAMC). The GRBC and REMC each contain approximately 10 proteins, and the PAMC approximately 5 proteins. The non-specific RNA-binding complex (MRP1/2) (Aphasizhev et al., 2003) interacts in an RNase-sensitive linkage to the GRBC and PAMC. Using cell disruption under cryogenic conditions, an interaction of mature edited mRNAs containing long poly A/U 3' tails with the large ribosomal subunit has also been detected (Aphasizheva et al., 2014). See Supplemental Tables S1–S4 for list of known protein components of editing complexes and mitoribosomes.

Previously, localization of RNA editing related components in trypanosomatids was reported to be localized either in "the kinetoplast region" or throughout the mitochondrion (Allen et al., 1998; Aphasizhev et al., 2003; McManus et al., 2001; Panigrahi et al., 2001). We showed previously that the RECC marker, REL1, localized in the kinetoplast region, as

did the accessory complex marker, REH1 (Li et al., 2011). In addition we reported a kinetoplast localization of two TAP-tagged mitochondrial ribosomal markers, S17 and L3. In this paper we investigate the localization of editing complexes in *L. tarentolae* in more detail using higher resolution indirect immunofluorescence of specific marker proteins with 3D reconstructions. We show that several editing complexes are localized in antipodal nodes adjacent to the kDNA disk and that these nodes are apparently separate from but associated with the minicircle repair-catenation nodes. We also show that mitochondrial ribosomes are also localized in kDNA disk-adjacent antipodal nodes separate from but closely associated to the editing complex and repair-catenation nodes.

2. Materials and methods

2.1 Antibodies for immunofluorescence

Mouse anti-REL1 monoclonal antibodies were prepared by the Caltech Monoclonal Facility. Rabbit anti-REH1 and mouse anti-RET1 polyclonal antibodies were generated by Covaris from recombinant proteins. Rabbit anti-FLAG antiserum was purchased from Pierce and mouse anti-FLAG antiserum was purchased from Rockland. Mouse anti-HA antiserum was purchased from Genscript and rabbit anti-HA antiserum was purchased from Rockland. Rabbit and goat anti-mouse IgG conjugated with Alexa Fluor 488 or 594 and goat anti-rabbit IgG conjugated with Alexa Fluor 488 or 594 were purchased from Life Technologies.

2.2 Leishmania culture

L. tarentolae strains UC and p10 were grown in Brain Heart Infusion (BHI) (Difco) at 27˚C with hemin added to 10 μg/ml (Simpson et al., 1970). The cells divide approximately every 6–9 hr and can reach densities of 100–400 million cells/ml. Cells were grown in 10 ml in T-flasks with gentle agitation at 27°C.

2.3 Construction of cell lines expressing tagged proteins

The following FLAG epitope-tagged editing proteins were expressed in *L. tarentolae* cells using episomal plasmids: REL1-SBP, MP44-SAP, MRP1-TAP, MRP2-TAP, L3-TAP, S17-TAP, and REH1-SAP. The p105 construct, which was obtained from Dr. Dan Ray, was HA epitope-tagged.

The pXG *Leishmania* expression vector (Ha et al., 1996) was modified for expression of SBP fusion proteins. A *Not* I site was generated in pXG through mutagenesis utilizing the QuickChange site-directed mutagenesis kit and the primer 5′ -TCCCCGGGGGAT**GCGGCCGC**AGATCCTCG −3′ . The SBP cassette and upstream insert was amplified from a modified TAP vector containing SBP in place of the CBP epitope sequence (Nelson and Simpson, unpublished results) using the primer pair 5′ -**CCCGGG**GCATGCGGGGCGTGCTAGCGCGTA −3′ , 5′ -GAAGATCT**GCGGCCGC**TTACTTGTCGTCGTCGTCCTTGTAGTCGGGCTCCCGCTGGCCCT −3′ (*Xma*I and *Not*I sites in bold) adding an additional 3′ FLAG epitope sequence (underlined). The *Xma*I and *Not*I digested sequence was inserted into the corresponding sites of the modified pXG vector to generate pXG-sbp-FLAG. The *Xma* I to *Xba* I fragment containing *Lt*REL1 cDNA was released from the *Lt*REL1-TAP vector (Aphasizhev et al.,

2003) and inserted into the modified pXG vector to generate pXG-*Lt*REL1-sbp-FLAG. *L. tarentolae* cells expressing *Lm*MP44-TAP (Li et al., 2009) under Geneticin selection were electroporated with pXG-*Lt*REL1-sbp-FLAG. Cell lines were selected on plates containing 200 μg/mL Geneticin and 100 μg/mL Hygromycin B and maintained in media containing 100 μg/mL Geneticin and 50 μg/mL Hygromycin B. These cells were transfected with the REL1-SBP-Flag vector to yield the KR7 strain. This strain was used to study the expression of epitope-tagged REL1.

2.4 Indirect Immunofluorescence and 3D reconstruction

The following incubation steps were carried out in a dark, humid chamber at room temperature. Cells were resuspended in 1% bovine serum albumin, 0.25 M sucrose, 20 mM Tris HCl (pH 7.9), pelleted and spread onto polylysine coated glass slides, dried rapidly and fixed for 5 min in methanol at 5°C. The cells were rehydrated by washing with PBS three times for 5 min and blocked with Background Buster (Innovex Biosciences). This was followed with three additional 5 min washes with PBS. Afterwards, the primary antibody (diluted 1:100 in 20% Goat serum-PBS) was added for 1 h. The cells were washed with PBST three times for 5 min and then the secondary antibody (diluted 1:500 in 20% goat serum-PBS) was added for 1 h. The cells were again washed with PBST three times for 5 min each. ProLong Gold antifade with DAPI (Invitrogen) was added and a glass cover slip was pressed on top. Images were taken using a Zeiss Axiomat microscope and Zeiss Axiovision 4.8 software. Z stacks of 20–24 ~0.2 μm slices were taken and 3D reconstructions created and deconvoluted with the Nearest Neighbor Algorithm using Axiovision.

UCSF Chimera (http://www.cgl.ucsf.edu/chimera/) was used for visualization of 3D images. The “surface” format selected in the Volume Viewer was used for ease of visualization. In general there is no generally accepted standard for thresholding the surface view in Chimera, even for cryoEM or crystal structures. It is especially difficult to find a “perfect” threshold for low resolution 3D images. But usually in a quite broad range of values, the size and shape of the displayed structure do not change greatly and out of this range the structure will disappear or lots of noise will come out abruptly. So any value in a broad range is fine if we can tell the size and shape of the structure. Another consideration that affected our consideration of a threshold was to achieve a structure equivalent to that seen in 2D immunofluorescent images of the same cells or to better visualize the tagged marker protein.

2.5 Cell cycle synchronization

L. tarentolae cells were kept in early-mid log phase (30–75 × 10^6 cells/ml) in BHI media, and hydroxyurea (HU) was added to a concentration of 200 μg/ml (Simpson et al. 1970). The cells were incubated for 10 h at 27 °C. Then cells were harvested, washed once and resuspended in fresh media without HU. A sample was taken immediately and additional samples were taken at 1 h intervals for 8 h from this time for slide preparation. Cells were kept at 27 °C with agitation during and after HU treatment for the entire length of the experiment.

3. Results

3.1 Localization of the RECC complex in antipodal nodes in wild type (wt) L. tarentolae

The RNA editing ligase 1 (REL1), which is a RECC component, was used as a marker protein for localization of this ~1 MDa complex. Indirect immunofluorescence of dried methanol-fixed wild type *L. tarentolae* cells using a monoclonal antibody against *L. tarentolae* REL1 and a secondary anti-mouse IgG antibody conjugated with a fluorescent dye shows the presence of antipodal nodes adjacent to the DAPI-stained kDNA disk. Fig. 1 shows several examples of bi-nodal REL1 configurations in wt *L. tarentolae*.

3.2 Mitochondrial ribosomes are also present in a nodal configuration

L. tarentolae cells were transformed with plasmids expressing TAP-tagged S17 and L3 mitochondrial ribosomal proteins. The S17 marker protein exhibits a bi-nodal configuration adjacent to the kDNA disk, as shown in the three representative cells in Fig. 2. The two antipodal nodes in each cell are boxed.

The TAP-tagged L3 expressing cells contain one or two nodes, and in the latter case, the nodes are often of different intensities. Panels 1–3 in Fig. 3A show examples of cells with a bi-nodal L3 configuration with nodes of equal intensities, panel 4 shows a cell with a single node adjacent to the kDNA disk, and panel 5 shows a bi-nodal L3 configuration with the nodes of different intensities. A densitometric scan of the two nodes in panel 5 is shown in Fig. 3B. The relative intensities of the two nodes vary between cells.

3.3 Several accessory editing complexes are also in nodal configurations

The GRBC accessory complexes show in the majority of the cells a bi-nodal configuration as shown in the three representative examples in Fig. 4. See Supplemental Fig. S3 for a field of 45 cells stained for GRBC. Thirty six of these cells exhibit two antipodal nodes, which are shown boxed. Seven examples of single node configurations are circled, and two examples of bi-nodal configurations in which the nodes are different intensities are in triangles.

The antipodal node configuration is also seen for RET1 as shown for four examples in Fig. 5. RET1 is a marker for the RET1 3’ TUTase accessory complex. As in the case of the GRBC complexes in Figs. 4 and Supplemental Fig. S3, the majority of the cells exhibit the antipodal node configuration. In Fig. S4, 71 cells show clearly identifiable 2 RET1 nodes (boxes) and 11 cells show a single node (circles). Cell outlines are not seen in this image due to the absence of phase contrast.

The fact that the RECC, GRBC and RET1 show nodal localizations in almost all cells in the asynchronous cultures used for these experiments suggest that the kDNA disk-associated nodes are not cell cycle-dependent as is the case for previously observed gap repair-catenation antipodal nodes (Jensen and Englund, 2012).

3.4 Bilateral sheet configuration of editing proteins

Another type of localization is seen in transgenic KR7 cells expressing both SBP-tagged REL1 and TAP-tagged MP44 from transfected episomal plasmids (MP44 is a RECC component of unknown function). Use of the anti-REL1 monoclonal antibody revealed that, in the majority of cells, the RECC is distributed in the KR7 cells as a bilateral sheet covering both the distal (TAC side) and the proximal surfaces of the kDNA disk. Several representative examples are shown in Fig. 6A. The length of the kDNA disk-associated RECC sheets is approximately 1 μm.

A minority of KR7 cells show the nodal configuration of REL1, as shown in Fig. 6B. A field of KR7 cells probed with anti-REL1 is shown in Supplemental Figs. S5A–C. In Fig. S5, Fig. 13 cells clearly showed REL1 (RECC) in a bilateral sheet configuration. This is a minimal estimate since visualization of the sheet configuration depends heavily on sample preparation and also on the precise focal plane imaged. A nodal configuration, as in wt cells, can be seen in a few cells in Fig. S5C (circled).

The RECC sheets occur in almost all KR7 cells in the population to varying extents. This can be seen in Supplemental Fig. S5A in which only the anti-REL1 fluorescence was used for imaging. Although the use of an anti-REL1 antibody precludes distinguishing the tagged and endogenous REL1, it is likely that this variation is due to the overexpression of REL1 in a subset of cells.

An apparent interaction of the kDNA-associated RECC with RECC dispersed throughout the single mitochondrion can be seen by overexposing the image as shown in in Fig. 7. This can also be seen in Supplemental Fig. S5A above.

A bilateral sheet distribution also occurs in the case of two additional accessory complexes as shown in Fig. 8. The MRP1/2 (Aphasizhev et al., 2003) and REH1 (Li et al., 2011) complexes, both of which were previously shown to be RNA-linked to RECC (Aphasizhev et al., 2003), exhibit a unilateral or bilateral sheet configuration. In addition, it appears that the kDNA disk-associated REH1 complexes are also linked to dispersed REH1 material. Since the MRP1/2 and REH1 were detected by specific antibodies, it is not possible to distinguish between the TAP-tagged MRP1/2 or the SAP-tagged REH1 and the endogenous proteins.

3.5 3D Reconstructions

A more detailed understanding of the geometry of the association between the nodes and sheets of editing complexes and the kDNA disk can be obtained by 3D reconstructions from multiple Z sections. Around 20–24 x ~0.2 μm z sections in a Zeiss Axiomat fluorescence microscope were used for reconstructions using Zeiss Axiovision software. Deconvolution was used to improve the resolution of the images which were then analyzed in 3D using the UCSF Chimera program. The 3D reconstruction of a representative RET1 nodal image in Fig. 9 shows clearly that the nodes are closely associated with the kDNA disk in an antipodal configuration. It should be emphasized that the relative sizes of the kDNA disks and the RET1 nodes are dependent on the surface thresholds set in Chimera, as discussed in Materials and Methods. This proviso holds for all the 3D reconstructions shown below.

Fig. 10 shows a 3D reconstruction of an example of the bilateral sheet configuration of REL1 (RECC) in KR7 cells. There is a narrow connection between the distal and proximal sheets and therefore we propose using the term, “horseshoe configuration”, to designate this morphology. The other end of the proximal sheet is connected to REL1 dispersed throughout the mitochondrion, as shown above. An example of a horseshoe configuration of another RECC component, TAP-tagged MP44, is shown in Fig. 11.

Several 3D reconstructions of the accessory complexes, MRP1/2-TAP and REH1-SAP, are shown in Fig. 12. The MRP1/2 proteins are in most cells in the form of a single distal sheet, which in a few cases is beginning to extend to the proximal side of the kDNA disk, suggesting that the editing complex material initially forms a distal sheet. The REH1 complex is usually present in a horseshoe configuration, with a connection of one end of the proximal sheet to dispersed REH1 complex material (shown above in Fig. 8).

3.6 Comparison of localization of different marker proteins in same cell

In order to determine if the editing complex nodes co-localize with the well-known minicircle gap repair-recatenation nodes, HA-tagged p105, a known component of the minicircle antipodal nodes, was co-expressed in cells transfected with an episomal plasmid for SBP-tagged REL1. Representative 3D reconstructions of REL1 and p105 nodes revealed distinct but closely associated RECC and gap repair-catenation nodes (Fig. 13A).

In addition, the relationship of GRBC nodes and REL1 nodes was analyzed in KR7 cells by immunofluorescence. As shown in the representative 3D image of two GRBC nodes with a single REL1 node in Fig. 13B, these two types of nodes are separate but closely associated with each other. Another 3D analysis of the relationship of GRBC nodes and the TAP-tagged L3 nodes is shown in Fig. 14. Again, the nodes are separate but closely associated.

3.6 Scission and formation of L3 nodes during the division and separation of daughter kDNA networks

The question arises as to the appearance of nodes during cell division when the kDNA disk undergoes scission. Fig. 15 shows a 3D reconstruction of TAP-tagged L3 nodes during the kDNA disk scission process in HU-synchronized cells. The extent of synchronization is shown in Fig. 15A. Several selected 2D images of this process are in Fig. 15B and several 3D reconstructions are in Fig. 15C. In S phase, the kDNA disk with two antipodal L3-TAP nodes lengthens and then undergoes scission to initiate cell division. Directly after scission of the kDNA disk, there is only a single L3-TAP node on one end of each daughter disk. This is rapidly followed by the appearance of a second node on each daughter kDNA disk. The presence of 2, 3 and 4 nodes can be seen in the 2D images.

4. Discussion

The organization of proteins involved in gap repair and catenation of replicated minicircles into kDNA disk-associated antipodal nodes has been known for some time, but the detailed structure of these nodes and the mechanism of interaction with the TAC fibrils and/or mitochondrial membranes is not understood. The proposed rotation of the kDNA disk during the replication process presents additional problems for any attachment model (Jensen and

Englund, 2012). The only other nodes of multiprotein minicircle replication complexes that have been described are two discrete structures localized on the distal side disk that contain the minicircle DNA binding protein, UMSBP, which is involved in replication of the randomly released closed minicircles during S phase.

We have demonstrated in this paper that most if not all of the U insertion/deletion RNA editing protein machiney is also localized in discrete antipodal nodes associated with the kDNA disk. We used antibodies against REL1, REH1, MRP1/2 and GRBC1/2 and also epitope-tagged episomal expressed marker proteins to detect the RECC as well as four accessory complexes which in some cases are RNA - linked to the RECC: MRP1/2, GRBC, RET1 and REH1. Some types of nodes are present throughout the cell cycle, such as REL1, GRBC and RET1, as shown by the presence of these in all cells of an asynchronous culture. This differs from the dynamic localization of mitochondrial DNA polymerases in *T. brucei* during the cell cycle (Concepcion-Acevedo et al., 2012) and the cell cycle localization of DNA ligases kα and kβ in *Crithidia*, and p105 in *T. brucei*. We also observed that, during the *Leishmania* cell cycle, the initial daughter kDNA disk scission products both lack one peripheral node which is then rapidly reconstituted for each disk. A similar observation was previously reported for the Topo II protein in *C. fasciculata* (Johnson and Englund, 1998). This absence of one node after kinetoplast division and its reconstitution probably explains our observations of two antipodal nodes of different intensities (Fig. 4): the less intense node may represent the recently reconstituted node after division. See Supplemental Tables S1–S4 for a listing of known protein components of editing complexes.

We also showed that in some cases in cells which are transfected with episomal plasmids expressing tagged editing proteins, the organization of the complexes changes into sheets which extend over one or two faces of the kDNA disk and are connected by a narrow neck resulting in a horse-shoe configuration. The other end of the proximal sheet opposite the connecting neck is continuous with editing complexes dispersed throughout the single mitochondrion indicating that only a portion of the editing complexes have coalesced into kDNA - associated sheets.

We saw a bilateral sheet horseshoe configuration for REL1 and MP44 (RECC) and also the REH1 accessory complex, and a mainly single distal sheet configuration for the MRP1/2 accessory complex. The localization of LIG kβ was previously reported as mainly nodal but not overlapping with that of Topo II, suggesting that these proteins may be contained in separate but associated complexes (Downey et al., 2004). LIG kβ also showed localization on both sides of the kDNA disk in a minority of cells, and the histone H1- like protein, Kap4, (Xu et al., 1996) and the mitochondrial helicase, TbPIF8 (Wang et al., 2012) both exhibited sheet-like configurations.

Overexpression cannot be the sole factor in determining the presence of the bilateral sheet configuration since the LIG kβ, TbPIF8 and Kap4 proteins were not overexpressed. On the other hand, TAP-tagged L3 and S17 mitochondrial ribosomal proteins expressed in *L tarentolae* from transfected episomal plasmids only appeared in antipodal nodes, but the extent of expression was not measured.

The most parsimonious model is that multiprotein editing protein complexes initially coalesce into spherical nodes associated at the edge of the kDNA disk, similar to the configuration of proteins involved in gap-repair and catenation of newly replicated minicircles into the edge of the rotating network (Jensen and Englund, 2012; Klingbeil and Englund, 2004). In some situations the nodes enlarge and finally merge into sheets attached to the surface of the kDNA disk, initially at the distal side as in the case of MRP1/2, and then extending to the proximal side via a narrow connection at one side of the disk. These sheets remain attached to editing complexes dispersed throughout the mitochondrion. The biological function of the sheet configuration, if any, is unknown. However even if this represents an artifact of overexpression, it has allowed a better understanding of the architecture of the dynamic interaction of editing complexes with the network of catenated minicircles. And in the case of the Topo II that probably releases randomly located covalently closed non-replicated minicircles from catenation on the distal side, a sheet-like localization is probably biologically functional.

By using antibodies specific for the RECC and gap repair-catenation editing proteins, we showed that the editing complex nodes were distinct from but closely associated with the minicircle gap repair-catenation nodes. This is also the case for RECC nodes and GRBC accessory complex nodes. The close association of the different nodes involved in minicircle replication and those involved in editing of kinetoplast maxicircle transcripts may reflect a functional linkage between the different node types or may result from an association of both types with the periphery of the kDNA disk and possibly with the TAC fibrillar network.

Another interesting observation is the existence of antipodal nodal concentrations of mitochondrial ribosomal large and small subunits and probably entire monosomes that are associated with editing complex nodes. The ribosomal nodes are separate from but closely associated with the GRBC nodes. While we did not examine the co-localization of the ribosomal and either RECC or gap repair-catenation nodes, the antipodal distributions of these features at the kDNA disk may suggest a functional relationship between these structures which may be related to the RNase sensitive ~40S editosomes (Osato et al., 2009) that contain at least 4 classes of multiprotein complexes, as was demonstrated by blue native gels and by co-immunoprecipitation, mass spectrometry and yeast two-hybrid analysis (Aphasizheva et al., 2014). Furthermore, an interaction of mature edited mRNAs with long 3’ A/U tails and mitoribosomes together with editing complexes has been detected biochemically in *T. brucei* by cell breakage under cryogenic conditions (Aphasizheva et al., 2014). It is unlikely that either the ~40S editosome or the putative larger complexes associated with mitoribosomes have been identified in this paper. Indeed, our imaging experiments show separation of the RECC and GRBC nodes, indicating that the majority of editing complexes may not exist as larger assemblies with GRBC auxiliary complexes. It is difficult however to access the effect of the sample preparation conditions on stability of the larger complexes.

In any case, the concentration of multiprotein editing complexes and mitoribosomes into nodes that are associated with the kDNA disk and with each other may prove functionally significant in increasing the efficiency of RNA editing and translation in terms of rotation of

the kDNA disk during minicircle replication and catenation exposing nascent pre-edited maxicircle transcripts to high concentrations of editing enzymes and mitoribosomes for editing and subsequent translation.

Supplementary Material

Refer to Web version on PubMed Central for supplementary material.

ACKNOWLEDGEMENTS

We thank Peter Bradley for kindly allowing us to use his Zeiss Axiomat fluorescent microscope and Dan Ray for supplying the HA-tagged p105 expression plasmid. Chimera was developed by the Resource for Biocomputing, Visualization and Informatics at the University of California, San Francisco. This work was supported in part by research grants from the National Institutes of Health (AI90102 to LS, AI101057 to RA and AI088292 to DM).

Abbreviations

gRNA	guide RNA
kDNA	kinetoplast DNA
RECC	RNA editing core complex
RET1	RNA editing TUTase 1
REH1	RNA editing helicase 1
REMC	RNA editing mediator complex
TAC	tripartite attachment complex
RESC	RNA editing substrate binding complex
GRBC	gRNA binding complex
RENC	RNA editing mediator complex
PAMC	polyadenylation mediator complex
REL1	RNA editing ligase 1
MRP1/2	mitochondrial RNA binding proteins 1 and 2
TAP	tandem affinity purification
U	uridylate
UMSBP	universal minicircle DNA binding protein

REFERENCES

Abu-Elneel K, Robinson DR, Drew ME, Englund PT, Shlomai J. Intramitochondrial localization of universal minicircle sequence-binding protein, a trypanosomatid protein that binds kinetoplast minicircle replication origins. The Journal of cell biology. 2001; 153:725–734. [PubMed: 11352934]

Alexeieff A. Sur la fonction glycoplastique du kinetoplaste (=kinetonucleus)chez les flagellates. C.R. Soc Biol. 1917; 80:512.

Allen TE, Heidmann S, Reed R, Myler PJ, Goringer HU, Stuart KD. Association of guide RNA binding protein gBP21 with active RNA editing complexes in Trypanosoma brucei. Mol Cell Biol. 1998; 18:6014–6022. [PubMed: 9742118]

Aphasizhev R, Aphasizheva I. Mitochondrial RNA processing in trypanosomes. Res Microbiol. 2011; 162:655–663. [PubMed: 21596134]

Aphasizhev R, Aphasizheva I. Mitochondrial RNA editing in trypanosomes: small RNAs in control. Biochimie. 2014; 100:125–131. [PubMed: 24440637]

Aphasizhev R, Aphasizheva I, Nelson RE, Simpson L. A 100-kD complex of two RNA-binding proteins from mitochondria of Leishmania tarentolae catalyzes RNA annealing and interacts with several RNA editing components. RNA. 2003; 9:62–76. [PubMed: 12554877]

Aphasizheva I, Zhang L, Wang X, Kaake RM, Huang L, Monti S, Aphasizhev R. RNA binding and core complexes constitute the u-insertion/deletion editosome. Mol Cell Biol. 2014; 34:4329–4342. [PubMed: 25225332]

Basile G, Peticca M. Recombinant protein expression in Leishmania tarentolae. Mol Biotechnol. 2009; 43:273–278. [PubMed: 19779853]

Beverley SM, Clayton CE. Transfection of Leishmania and Trypanosoma brucei by electroporation. Methods Mol.Biol. 1993; 21:333–348. [PubMed: 8220725]

Bonhivers M, Landrein N, Decossas M, Robinson DR. A monoclonal antibody marker for the exclusion-zone filaments of Trypanosoma brucei. Parasites & vectors. 2008; 1:21. [PubMed: 18616805]

Breitling R, Klingner S, Callewaert N, Pietrucha R, Geyer A, Ehrlich G, Hartung R, Muller A, Contreras R, Beverley SM, Alexandrov K. Non-pathogenic trypanosomatid protozoa as a platform for protein research and production. Protein Expr.Purif. 2002; 25:209–218. [PubMed: 12135552]

Bruhn DF, Sammartino MP, Klingbeil MM. Three mitochondrial DNA polymerases are essential for kinetoplast DNA replication and survival of bloodstream form Trypanosoma brucei. Eukaryot Cell. 2011; 10:734–743. [PubMed: 21531873]

Concepcion-Acevedo J, Luo J, Klingbeil MM. Dynamic localization of Trypanosoma brucei mitochondrial DNA polymerase ID. Eukaryot Cell. 2012; 11:844–855. [PubMed: 22286095]

Couvreur B. Whole-cell antigenicity data support sequence-based kinetoplastid taxonomy. Mem Inst Oswaldo Cruz. 2013; 108:248–250. [PubMed: 23579809]

Dortay H, Mueller-Roeber B. A highly efficient pipeline for protein expression in Leishmania tarentolae using infrared fluorescence protein as marker. Microb Cell Fact. 2010; 9:29. [PubMed: 20459748]

Downey N, Sinha KM, Hines JC, Ray DS. Mitochondrial DNA ligase in Crithidia fasciculata. Proc. Natl. Acad. Sci. U.S.A. 2004; 101:4361–4366. [PubMed: 15070723]

Engel ML, Ray DS. The kinetoplast structure-specific endonuclease I is related to the 5’ exo/endonuclease domain of bacterial DNA polymerase I and colocalizes with the kinetoplast topoisomerase II and DNA polymerase á during replication. Proc. Natl. Acad. Sci. USA. 1999; 96:8455–8460. [PubMed: 10411896]

Fraga J, Montalvo AM, De Doncker S, Dujardin JC, Van der Auwera G. Phylogeny of Leishmania species based on the heat-shock protein 70 gene. Infect Genet Evol. 2010; 10:238–245. [PubMed: 19913110]

Fritsche C, Sitz M, Weiland N, Breitling R, Pohl HD. Characterization of the growth behavior of Leishmania tarentolae: a new expression system for recombinant proteins. J Basic Microbiol. 2007; 47:384–393. [PubMed: 17910102]

Golas MM, Bohm C, Sander B, Effenberger K, Brecht M, Stark H, Goringer HU. Snapshots of the RNA editing machine in trypanosomes captured at different assembly stages in vivo. The EMBO journal. 2009; 28:766–778. [PubMed: 19197238]

Gomez-Eichelmann MC, Holz G Jr, Beach D, Simpson AM, Simpson L. Comparison of several lizard Leishmania species and strains in terms of kinetoplast minicircle and maxicircle DNA sequences, nuclear chromosomes, and membrane lipids. Mol.Biochem.Parasitology. 1988; 27:143–158.

Goyard S, Beverley SM. Blasticidin resistance: a new independent marker for stable transfection of Leishmania Mol. Biochem. Parasitol. 2000; 108:249–252.

Ha DS, Schwarz JK, Turco SJ, Beverley SM. Use of the green fluorescent protein as a marker in transfected Leishmania Mol. Biochem. Parasitol. 1996; 77:57–64.

Hashimi H, Zikova A, Panigrahi AK, Stuart KD, Lukes J. TbRGG1, an essential protein involved in kinetoplastid RNA metabolism that is associated with a novel multiprotein complex. RNA. 2008; 14:970–980. [PubMed: 18369185]

Hines JC, Ray DS. A mitochondrial DNA primase is essential for cell growth and kinetoplast DNA replication in Trypanosoma brucei. Mol Cell Biol. 2010; 30:1319–1328. [PubMed: 20065037]

Hines JC, Ray DS. A second mitochondrial DNA primase is essential for cell growth and kinetoplast minicircle DNA replication in Trypanosoma brucei. Eukaryot Cell. 2011; 10:445–454. [PubMed: 21257796]

Jensen RE, Englund PT. Network news: the replication of kinetoplast DNA. Annu Rev Microbiol. 2012; 66:473–491. [PubMed: 22994497]

Johnson CE, Englund PT. Changes in organization of Crithidia fasciculata kinetoplast DNA replication proteins during the cell cycle. J. Cell Biol. 1998; 143:911–919. [PubMed: 9817750]

Kang X, Gao G, Rogers K, Falick AM, Zhou S, Simpson L. Reconstitution of full-round uridine-deletion RNA editing with three recombinant proteins. Proc. Natl. Acad. Sci. U.S.A. 2006; 103:13944–13949. [PubMed: 16963561]

Klatt S, Konthur Z. Secretory signal peptide modification for optimized antibody-fragment expression-secretion in Leishmania tarentolae. Microb Cell Fact. 2012; 11:97. [PubMed: 22830363]

Klingbeil MM, Englund PT. Closing the gaps in kinetoplast DNA network replication. Proc.Natl.Acad.Sci.U.S.A. 2004; 101:4333–4334. [PubMed: 15070715]

Klingbeil MM, Motyka SA, Englund PT. Multiple mitochondrial DNA polymerases in Trypanosoma brucei. Mol Cell. 2002; 10:175–186. [PubMed: 12150917]

Kovtun O, Mureev S, Johnston W, Alexandrov K. Towards the construction of expressed proteomes using a Leishmania tarentolae based cell-free expression system. PloS one. 2010; 5:14388.

Kushnir S, Cirstea IC, Basiliya L, Lupilova N, Breitling R, Alexandrov K. Artificial linear episome-based protein expression system for protozoon Leishmania tarentolae. Mol Biochem Parasitol. 2011; 176:69–79. [PubMed: 21167214]

Kushnir S, Gase K, Breitling R, Alexandrov K. Development of an inducible protein expression system based on the protozoan host Leishmania tarentolae. Protein Expr Purif. 2005; 42:37–46. [PubMed: 15939291]

Lacomble S, Vaughan S, Deghelt M, Moreira-Leite FF, Gull K. A Trypanosoma brucei protein required for maintenance of the flagellum attachment zone and flagellar pocket ER domains. Protist. 2012; 163:602–615. [PubMed: 22186015]

Li F, Ge P, Hui W, Atanasov A, Rogers K, Guo Q, Osato D, Falick AM, Zhou H, Simpson L. Structure of the Core Editing Complex (L-Complex) Involved in Uridine Insertion/Deletion RNA Editing in Trypanosomatid Mitochondria. Proc. Natl. Acad. Sci. USA. 2009

Li F, Herrera J, Zhou S, Maslov DA, Simpson L. Trypanosome REH1 is an RNA helicase involved with the 3'-5' polarity of multiple gRNA-guided uridine insertion/deletion RNA editing. Proc Natl Acad Sci U S A. 2011; 108:3542–3547. [PubMed: 21321231]

Li Y, Sun Y, Hines JC, Ray DS. Identification of new kinetoplast DNA replication proteins in trypanosomatids based on predicted S-phase expression and mitochondrial targeting. Eukaryot Cell. 2007; 6:2303–2310. [PubMed: 17965251]

Liu B, Molina H, Kalume D, Pandey A, Griffith JD, Englund PT. Role of p38 in replication of Trypanosoma brucei kinetoplast DNA. Mol Cell Biol. 2006; 26:5382–5393. [PubMed: 16809774]

Liu B, Wang J, Yildirir G, Englund PT. TbPIF5 is a Trypanosoma brucei mitochondrial DNA helicase involved in processing of minicircle Okazaki fragments. PLoS Pathog. 2009; 5:1000589.

Liu B, Yildirir G, Wang J, Tolun G, Griffith JD, Englund PT. TbPIF1, a Trypanosoma brucei mitochondrial DNA helicase, is essential for kinetoplast minicircle replication. J Biol Chem. 2010; 285:7056–7066. [PubMed: 20042610]

Maslov DA, Simpson L. The polarity of editing within a multiple gRNA-mediated domain is due to formation of anchors for upstream gRNAs by downstream editing. Cell. 1992; 70:459–467. [PubMed: 1379519]

McManus MT, Shimamura M, Grams J, Hajduk SL. Identification of candidate mitochondrial RNA editing ligases from Trypanosoma brucei. RNA. 2001; 7:167–175. [PubMed: 11233974]

Melendy T, Sheline C, Ray D. Localization of a type II DNA topoisomerase to two sites at the periphery of the kinetoplast DNA of Crithidia fasciculata. Cell. 1988; 56:1083–1088. [PubMed: 2849507]

Miles AA. Muriel Robertson, 1883–1973. Journal of general microbiology. 1976; 95:1–8. [PubMed: 784900]

Ogbadoyi EO, Robinson DR, Gull K. A high-order trans-membrane structural linkage is responsible for mitochondrial genome positioning and segregation by flagellar basal bodies in trypanosomes. Molecular biology of the cell. 2003; 14:1769–1779. [PubMed: 12802053]

Onn I, Kapeller I, Abu-Elneel K, Shlomai J. Binding of the universal minicircle sequence binding protein at the kinetoplast DNA replication origin. J Biol Chem. 2006; 281:37468–37476. [PubMed: 17046830]

Osato D, Rogers K, Guo Q, Li F, Richmond G, Klug F, Simpson L. Uridine insertion/deletion RNA editing in trypanosomatid mitochondria: in search of the editosome. RNA. 2009; 15:1338–1344. [PubMed: 19447916]

Panigrahi AK, Gygi SP, Ernst NL, Igo RP, Palazzo SS, Schnaufer A, Weston DS, Carmean N, Salavati R, Aebersold R, Stuart KD. Association of two novel proteins, TbMP52 and TbMP48, with the Trypanosoma brucei RNA editing complex. Mol.Cell Biol. 2001; 21:380–389. [PubMed: 11134327]

Saxowsky TT, Choudhary G, Klingbeil MM, Englund PT. Trypanosoma brucei has two distinct mitochondrial DNA polymerase beta enzymes. J. Biol. Chem. 2003; 278:49095–49101. [PubMed: 12966090]

Schnarwiler F, Niemann M, Doiron N, Harsman A, Kaser S, Mani J, Chanfon A, Dewar CE, Oeljeklaus S, Jackson CB, Pusnik M, Schmidt O, Meisinger C, Hiller S, Warscheid B, Schnaufer AC, Ochsenreiter T, Schneider A. Trypanosomal TAC40 constitutes a novel subclass of mitochondrial beta-barrel proteins specialized in mitochondrial genome inheritance. Proc Natl Acad Sci U S A. 2014; 111:7624–7629. [PubMed: 24821793]

Simpson AG, Stevens JR, Lukes J. The evolution and diversity of kinetoplastid flagellates. Trends Parasitol. 2006; 22:168–174. [PubMed: 16504583]

Simpson L, da Silva AM. Isolation and characterization of kinetoplast DNA from Leishmania tarentolae. J. Mol. Biol. 1971; 56:443–473. [PubMed: 4324686]

Simpson L, Douglass SM, Lake JA, Pellegrini M, Li F. Comparison of the Mitochondrial Genomes and Steady State Transcriptomes of Two Strains of the Trypanosomatid Parasite, Leishmania tarentolae. PLoS Negl Trop Dis. 2015; 9:003841.

Simpson L, Simpson A, Wesley R. Replication of the kinetoplast DNA of Leishmania tarentolae and Crithidia fasciculata. Biochim.Biophys.Acta. 1974; 349:161–172. [PubMed: 4836350]

Sinha KM, Hines JC, Downey N, Ray DS. Mitochondrial DNA ligase in Crithidia fasciculata. Proc Natl Acad Sci U S A. 2004; 101:4361–4366. [PubMed: 15070723]

Sturm NR, Simpson L. Leishmania tarentolae minicircles of different sequence classes encode single guide RNAs located in the variable region approximately 150 bp from the conserved region. Nucleic Acids Res. 1991; 19:6277–6281. [PubMed: 1720240]

Taylor VM, Munoz DL, Cedeno DL, Velez ID, Jones MA, Robledo SM. Leishmania tarentolae: utility as an in vitro model for screening of antileishmanial agents. Exp Parasitol. 2010; 126:471–475. [PubMed: 20685203]

Wang J, Englund PT, Jensen RE. TbPIF8, a Trypanosoma brucei protein related to the yeast Pif1 helicase, is essential for cell viability and mitochondrial genome maintenance. Mol Microbiol. 2012; 83:471–485. [PubMed: 22220754]

Xu CW, Hines JC, Engel ML, Russell DG, Ray DS. Nucleus-encoded histone H1-like proteins are associated with kinetoplast DNA in the trypanosomatid Crithidia fasciculata. Mol.Cell Biol. 1996; 16:564–576. [PubMed: 8552084]

Zhao Z, Lindsay ME, Roy Chowdhury A, Robinson DR, Englund PT. p166, a link between the trypanosome mitochondrial DNA and flagellum, mediates genome segregation. The EMBO journal. 2008; 27:143–154. [PubMed: 18059470]

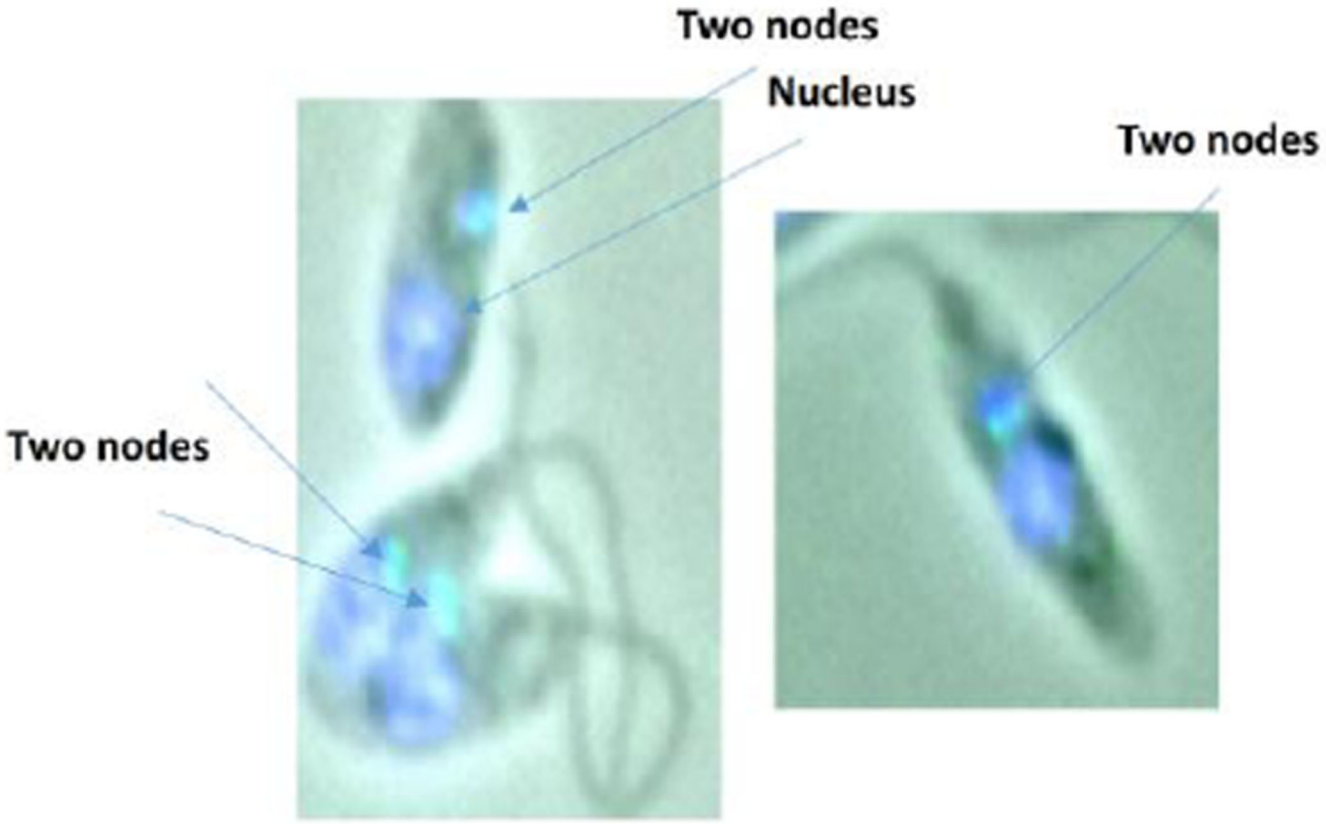

Fig. 1. Several examples of REL1 bi-nodal distribution in wild type *L. tarentolae*
A dividing cell is seen in the left panel.

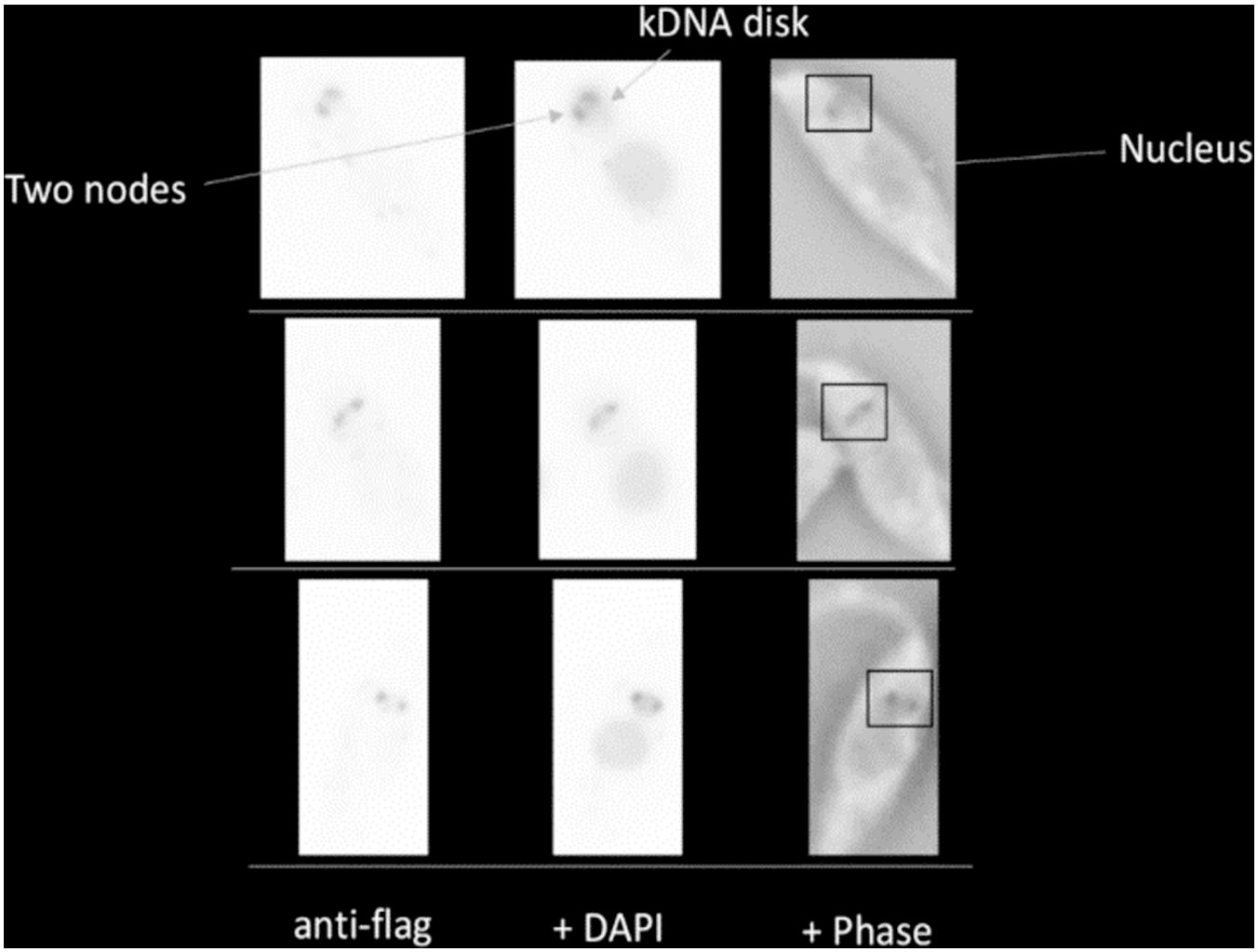

Fig. 2. Nodal configuration of TAP-tagged small subunit mitochondrial ribosomal protein S17

Three representative cells with a two antipodal node configuration of S17 are shown boxed in the right panels. The panels (left to right) show anti-flag antibody+anti-rabbit IgG coupled with red dye, same with DAPI, same with DAPI and phase contrast.

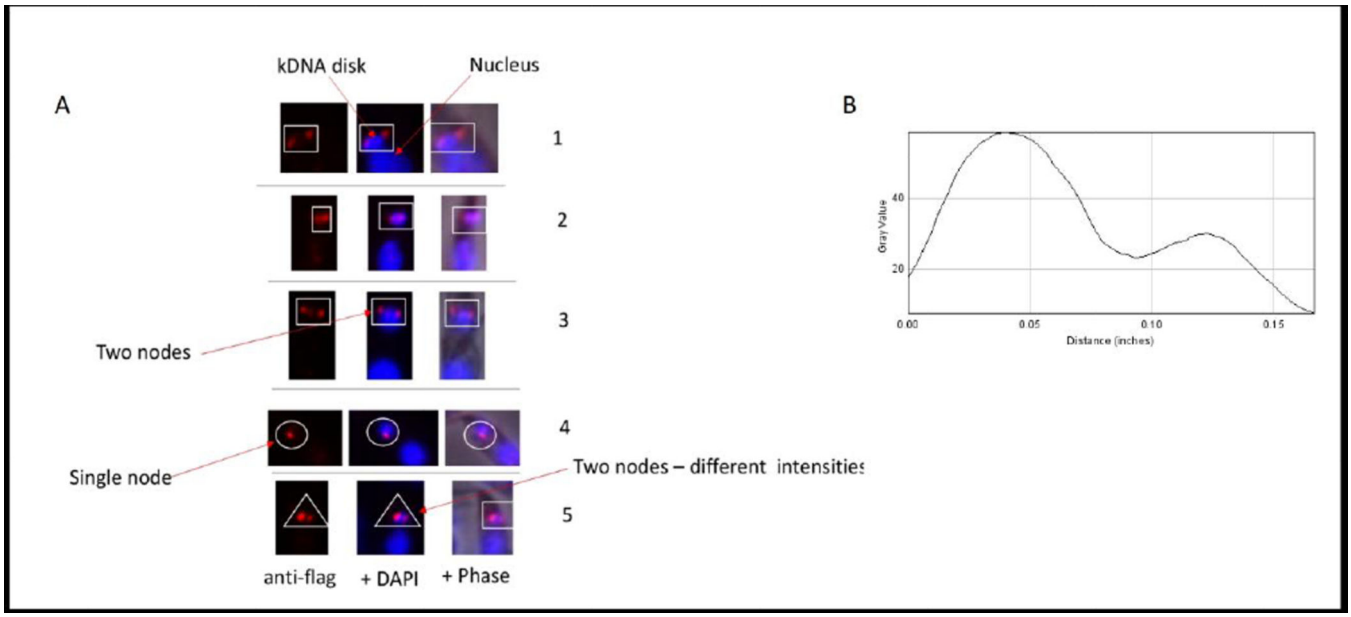

Fig. 3. Nodal configuration of TAP-tagged large subunit mitochondrial ribosomal protein L3

A. Three representative cells with a two node configuration are in panels 1–3. See Fig. 2 legend for details. Panel 4 shows a single node configuration and panel 5 shows two nodes of different intensities. B. Densitometric scan of two nodes in panel 5. Second node is 11% of first node.

Fig. 4. Bi-nodal configuration of GRBC complex

Cells dried on slide probed with anti-GRBC antibody and then with anti-rabbit IgG, and stained with DAPI. Only the anti-GRBC and DAPI are shown. No phase contrast.

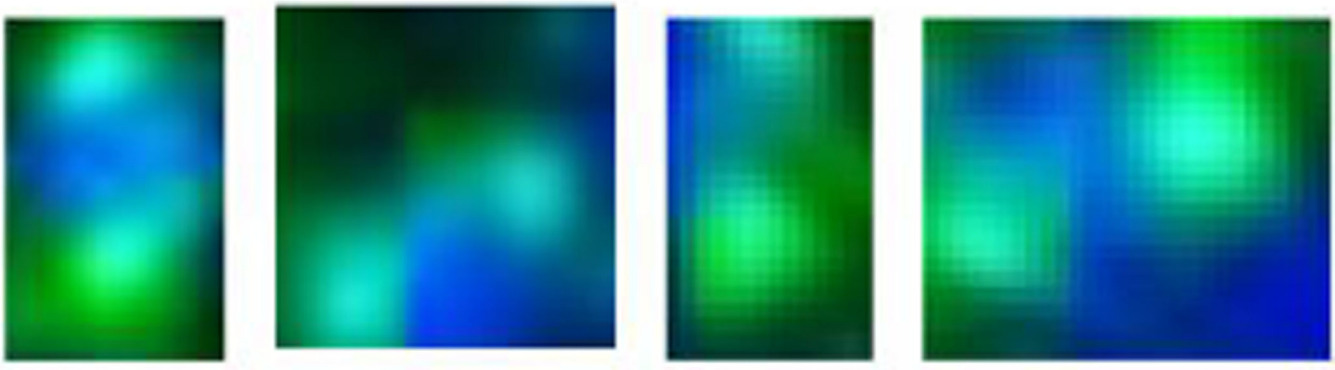

Fig. 5. Bi-nodal configuration of RET1 complexes

Cells dried and probed with anti-RET1 antibody, anti-rat IgG coupled with green dye and stained with DAPI. No phase contrast.

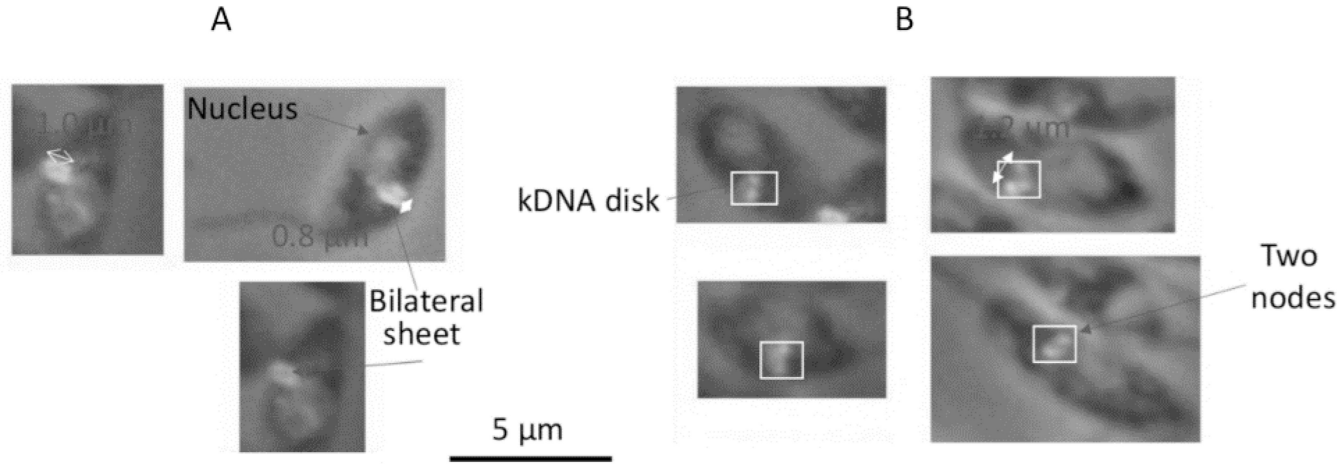

Fig. 6. Several examples of bilateral sheet configuration of REL1 and also several examples of the minor nodal configuration in KR7 cells

The dried cells were probed with anti-REL1 monoclonal antibody and then with anti-mouse IgG coupled with a green fluorescent dye and stained with DAPI. Cells imaged for REL1 fluorescence (green), DNA (blue) and phase contrast.

A. Bilateral sheet. B. Antipodal nodes. The scales were determined from a 5 µm scale bar.

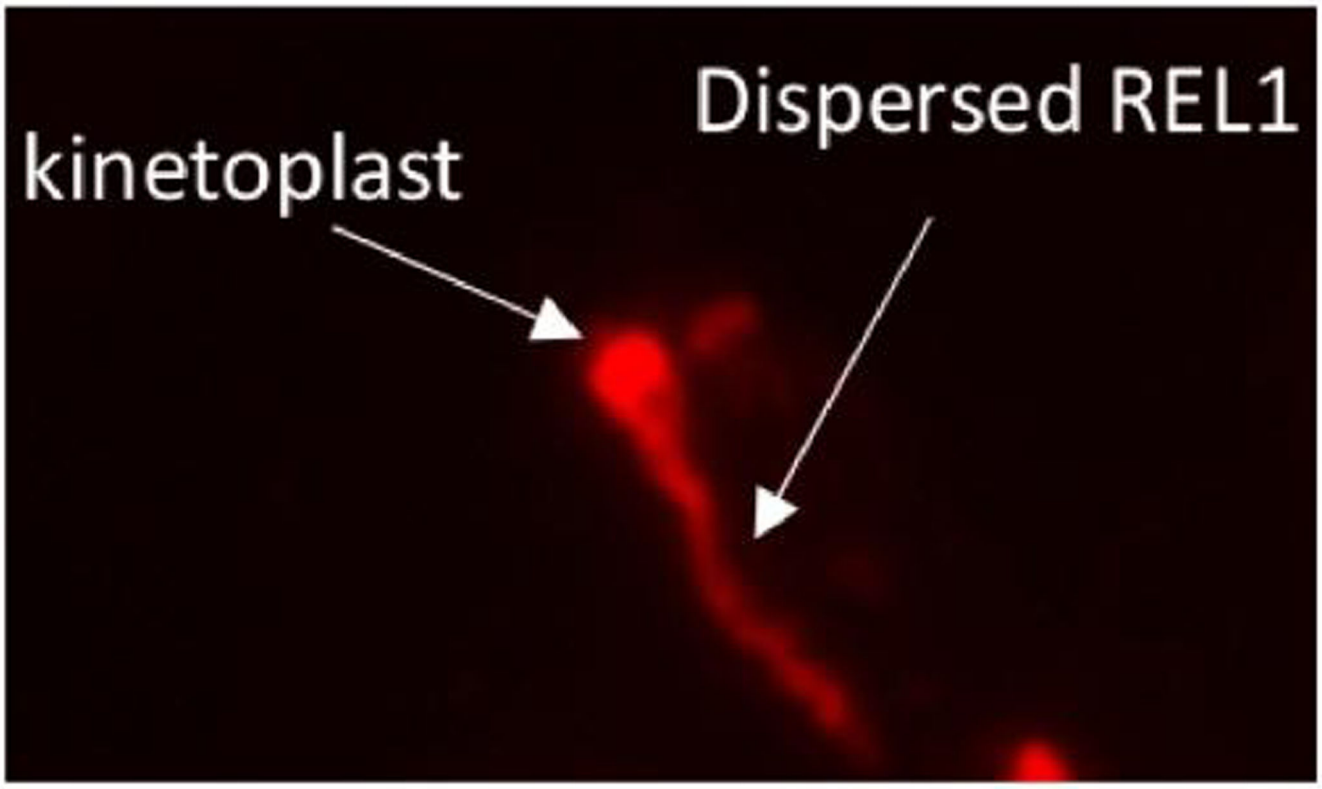

Fig. 7. Dispersed REL1

Overexposure of image of KR7 cells probed for REL1 (red) shows presence of REL1 dispersed throughout the single mitochondrion. The kinetoplast and dispersed REL1 are indicated by arrows.

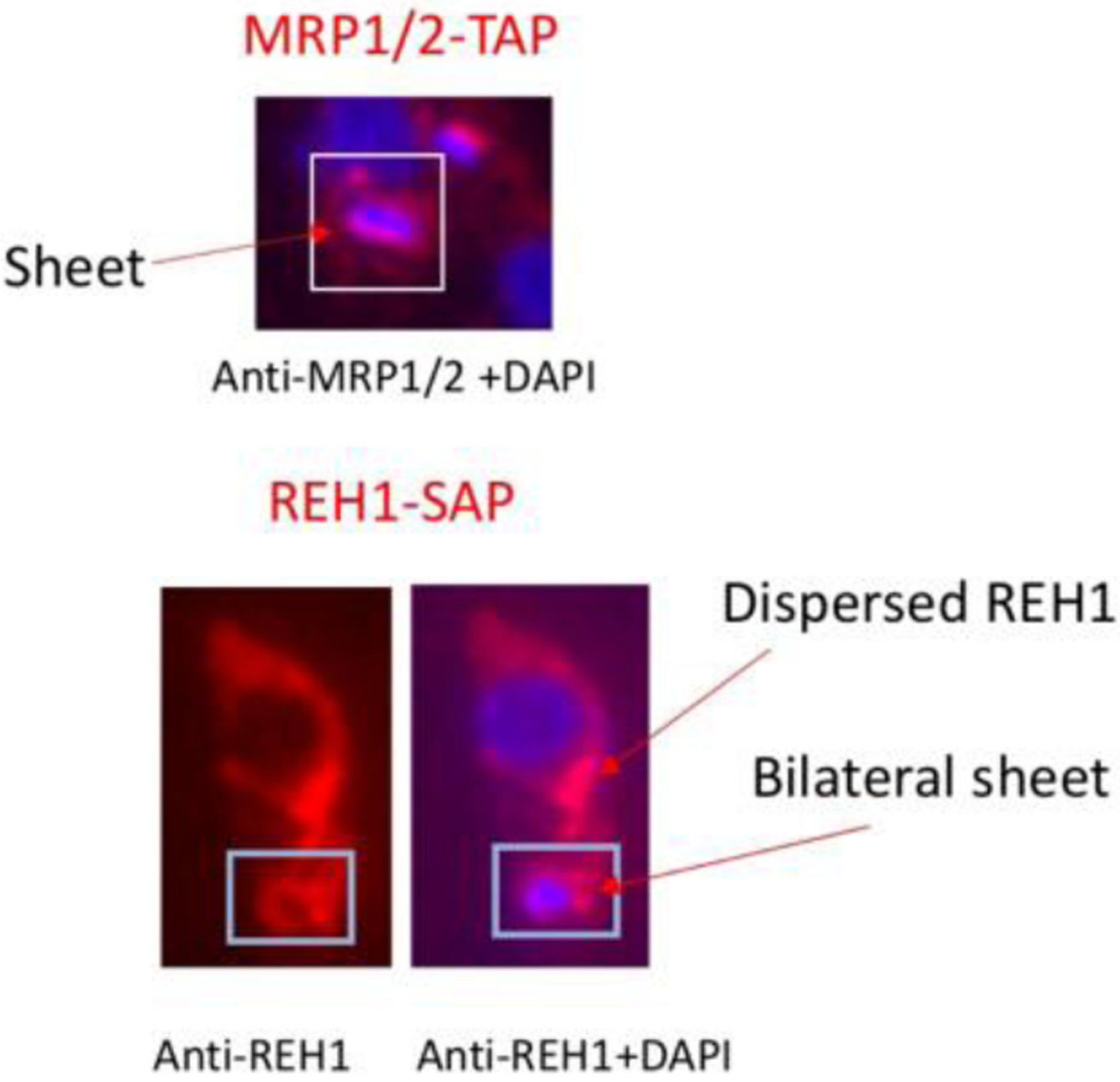

Fig. 8. Sheet configurations of MRP1/2 and REH1

Cells expressing TAP-tagged MRP1/2 and also cells expressing SAP-tagged REH1 were probed with antibodies against MRP1/2 and REH1. The sheet configuration of MRP1/2 and REH1 are indicated by boxes and arrows. It is not possible to distinguish between the tagged proteins or the endogenous proteins. Note the connection of the kinetoplast-associated REH1 to a high concentration of dispersed REH1.

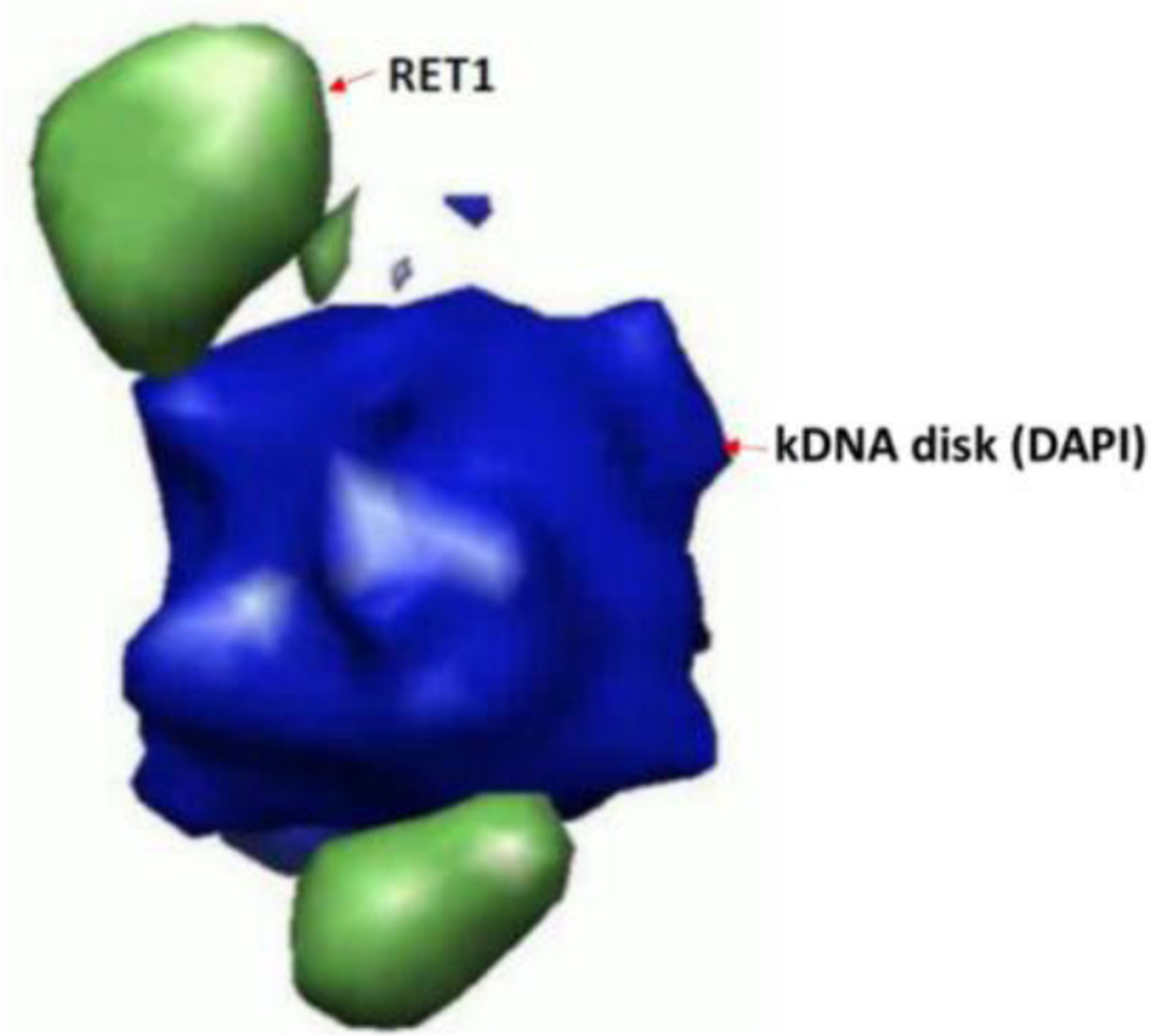

Fig. 9. 3D reconstruction of an example of the antipodal node configuration of RET1
The green RET1 nodes are closely associated with the blue kDNA disk.

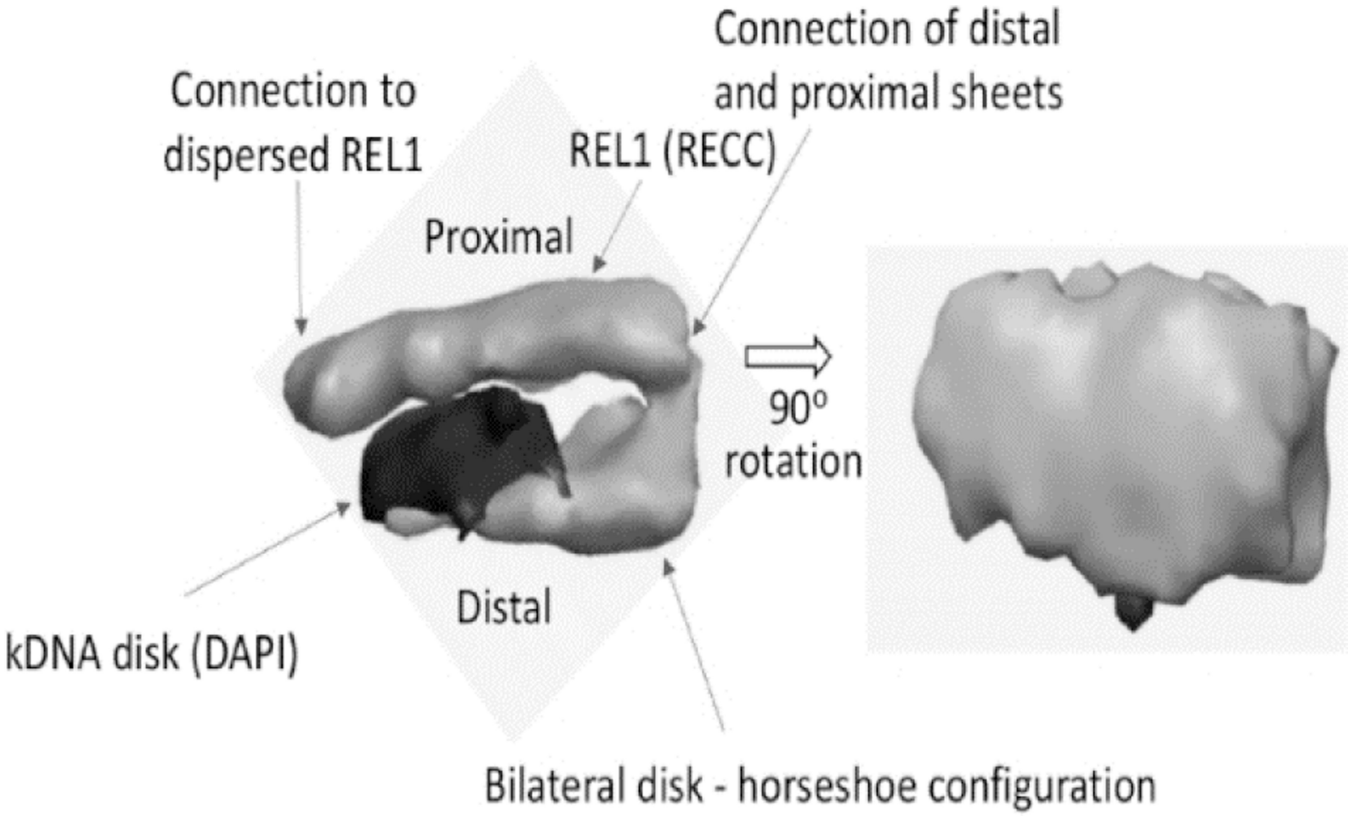

Fig. 10. 3D reconstruction of the REL1 "horseshoe configuration" in KR7 cells

The distal and proximal REL1 (green) sheets are connected at one end and the opposite end of the proximal sheet interacts with dispersed intra-mitochondrial REL1. Two images are shown rotated 90°.

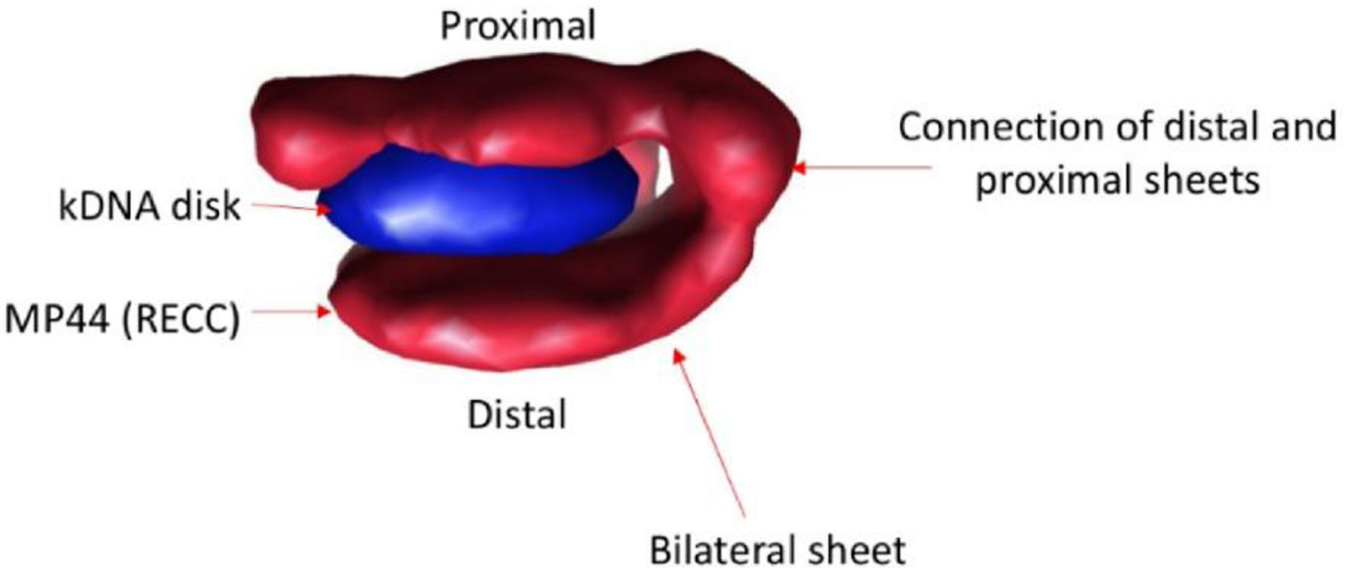

Fig. 11. 3D reconstruction of the MP44 "horseshoe configuration"

MP44 forms distal and proximal bilateral sheets connected at one end as in the case of REL1 in Fig. 10.

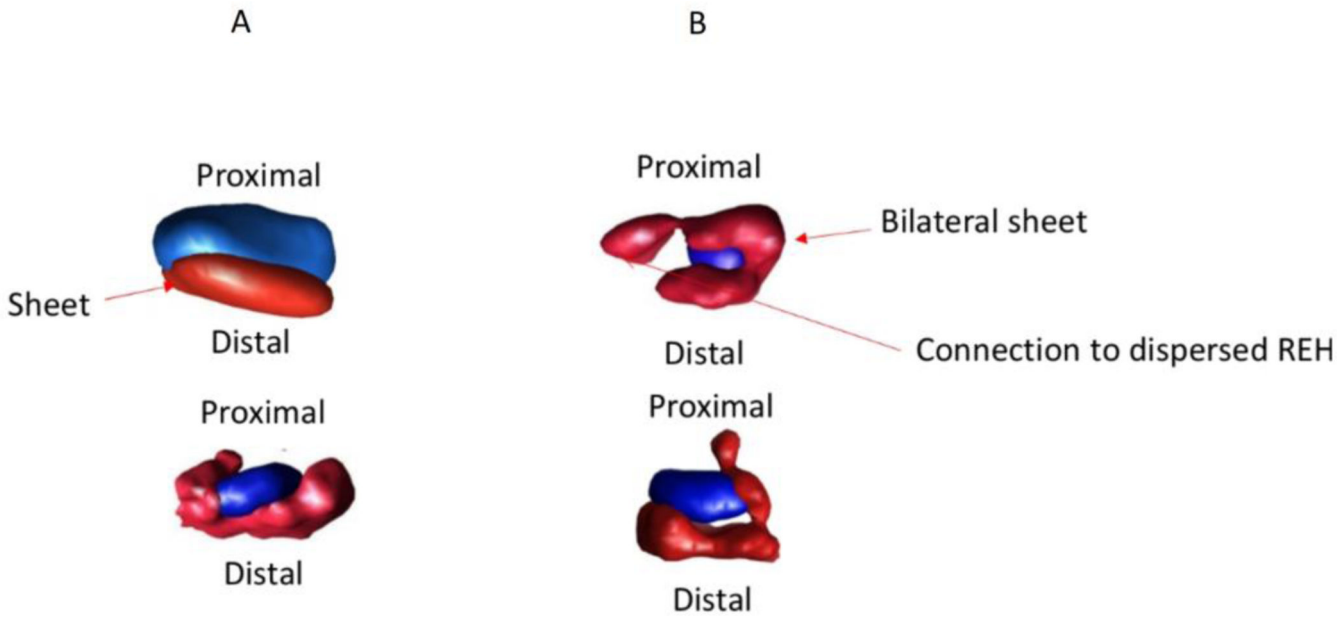

Fig. 12. 3D reconstructions of the MRP1/2 and the REH1 sheet configurations

A. The majority of the MRP1/2 configurations consisted of a single distal sheet as shown in the upper example. The lower image represents a possible intermediate where the sheet is extending to the proximal side of the kDNA disk. Note that since anti-MRP1/2 antibodies were used, it is not possible to distinguish between endogenous proteins and epitope tagged proteins. B. Two representative examples of three dimensional reconstructions of bilateral sheet REH1 configurations. The upper image shows a connection of the proximal sheet to dispersed REH1.

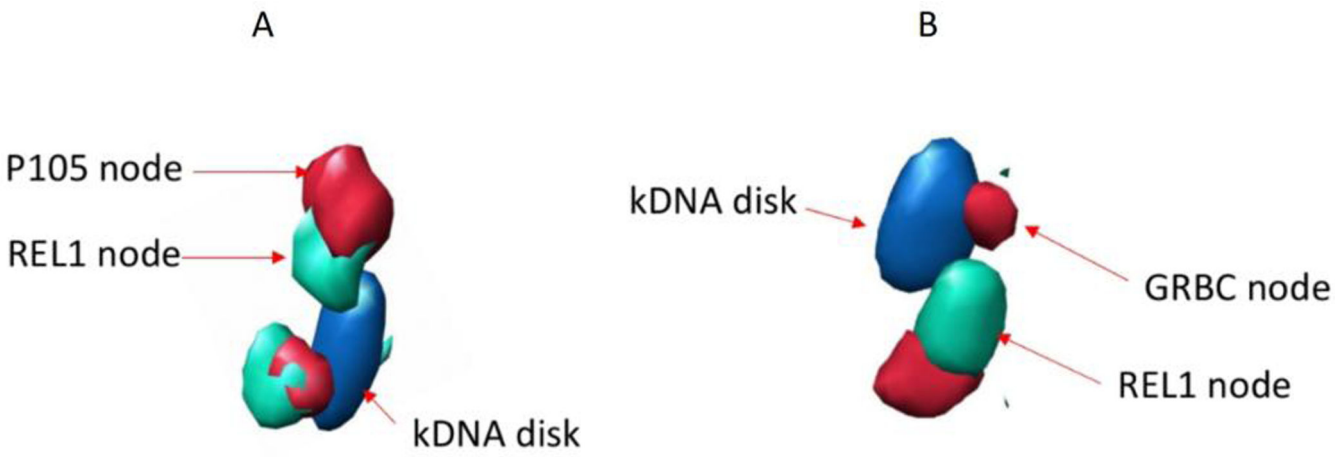

Fig. 13. Spatial relationship of REL1 nodes and repair-catenation nodes

A. A 3D reconstruction of co-expressed SBP-tagged REL1 and HA-tagged p105 (repair-catenation marker) probed with anti-REL1 antibodies (green) and anti-HA antibodies (red), and stained with DAPI (blue). B. 3D reconstruction of REL1 (green) and GRBC (red). The apparent non-antipodal localization of one GRBC node may be an artifact of sample preparation. Since anti-REL1 antibodies were used in both cases, it is not possible to distinguish SBP-tagged REL1 and endogenous REL1.

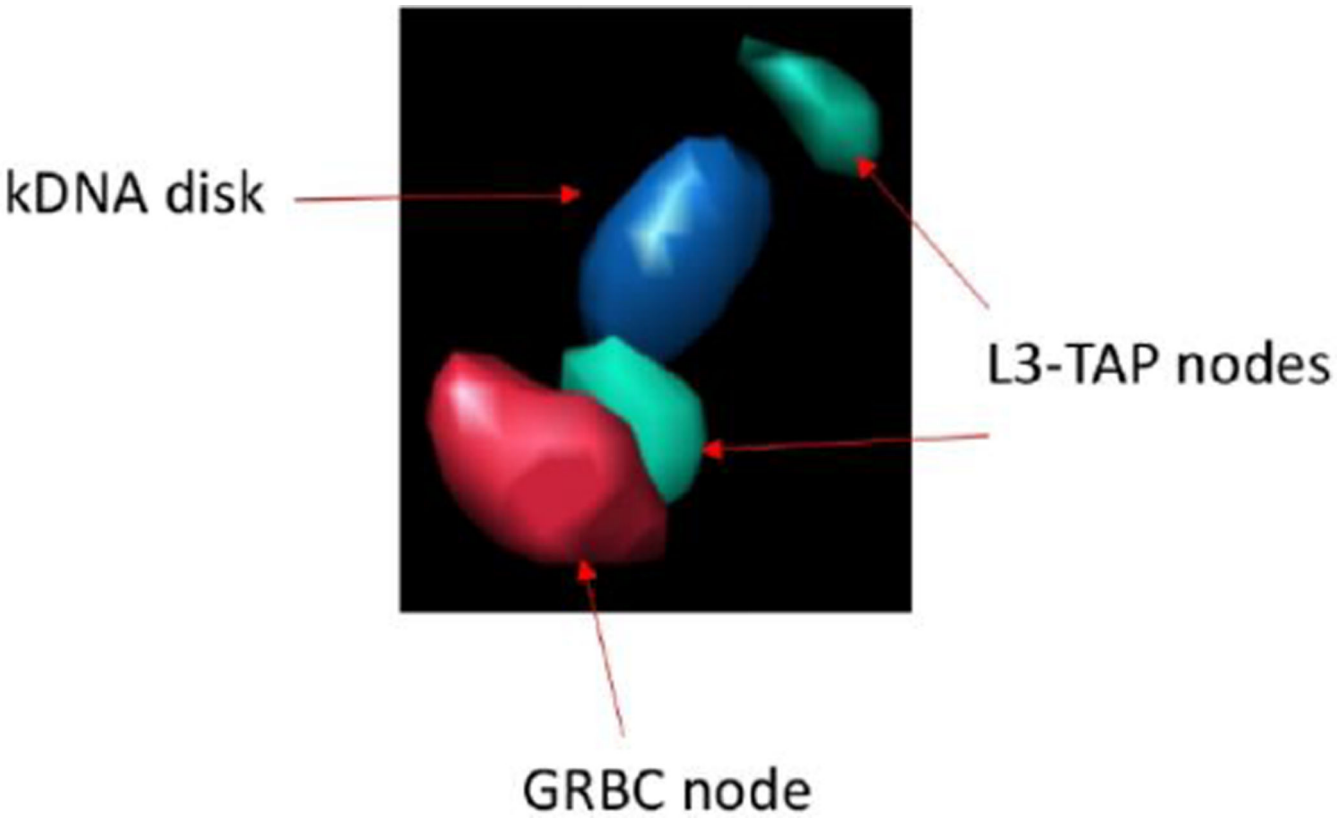

Fig. 14. 3D reconstruction of the relationship of L3 and GRBC nodes

Two antipodal TAP-tagged L3 nodes (green) are adjacent to the kDNA disk, and a single GRBC node (red) is closely opposed to one of the L3 nodes.

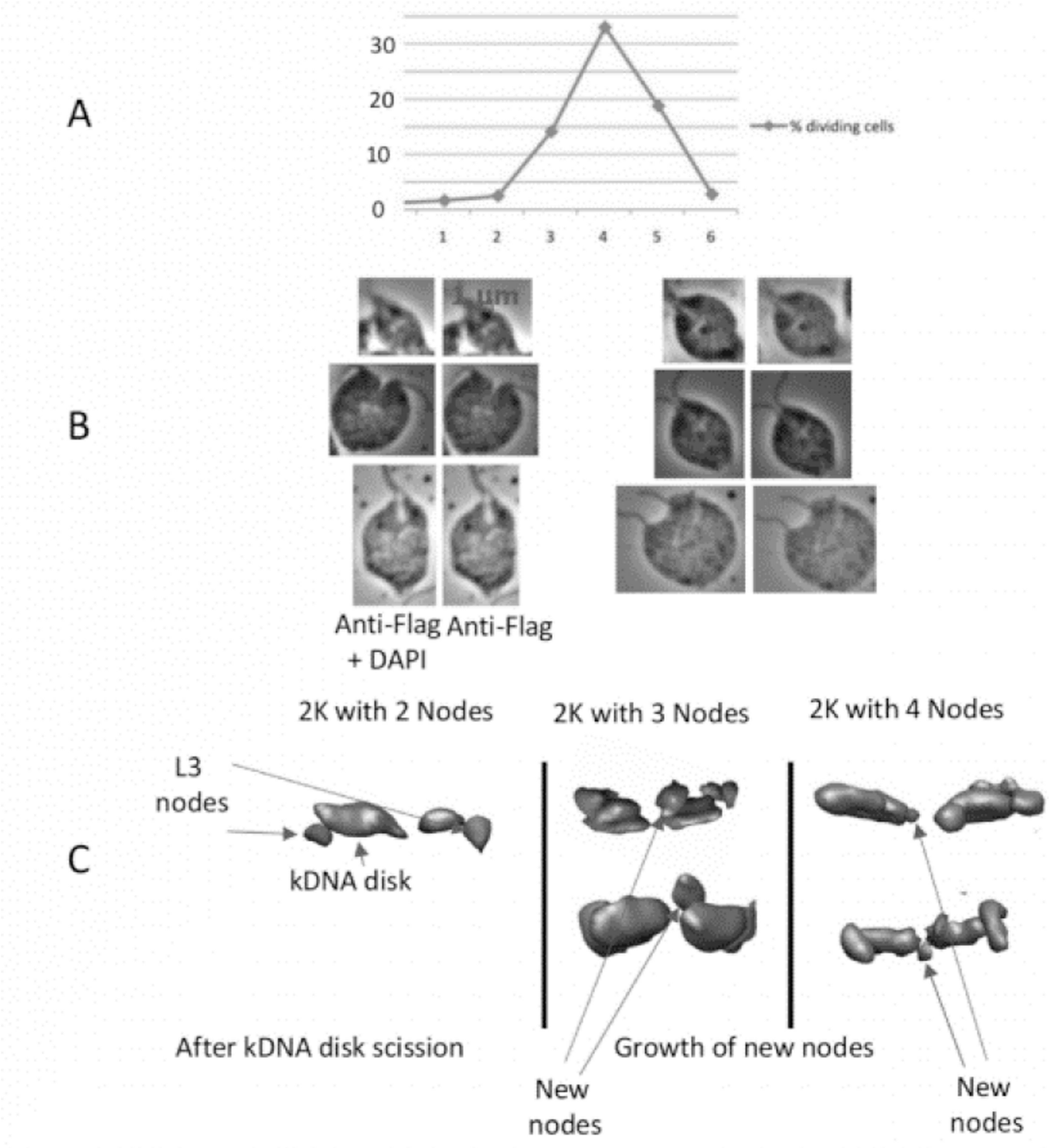

Fig. 15. 3D reconstructions of TAP-tagged L3 nodes during cell division

L. tarentolae cells expressing TAP-tagged L3 protein were synchronized by hydroxyurea inhibition, collected during the division phase and attached to slides for indirect immunofluorescence. Cells were probed with anti-flag antibodies for TAP-tagged L3 immunofluorescence (red) and stained with DAPI (blue). A. Graph showing peak of dividing cells 4 hr after removal of hydroxyurea. B. Two selected sequences of 2D images of dividing cells. C. Several selected 3D reconstructions of kDNA disks with L3 nodes. The left panel shows that immediately after scission of the kDNA disk there is no visible second

node. The middle panel shows two examples of the appearance of new nodes on the daughter kDNA disks. The right panel shows the appearance of a second node on the daughter kDNA disks.